Journal of Cell Science 106, 555-564 (1993)
Printed in Great Britain © The Company of Biologists Limited 1993

Organelle movements in the wild type and wall-less fz;sg;os-1 mutants of *Neurospora crassa* are mediated by cytoplasmic microtubules

Gero Steinberg* and Manfred Schliwa

Institute for Cell Biology, Ludwig-Maximilians-University Munich, Schillerstraße 42, 80336 München, Germany

*Author for correspondence

SUMMARY

The cellular basis of organelle transport in filamentous fungi is still unresolved. Here we have studied the intracellular movement of mitochondria and other organelles in the fungus *Neurospora crassa*. Four different model systems were employed: hyphae, protoplasts, a cell wall-less mutant, and experimentally generated small, flattened cell fragments of the mutant cells. Organelle movements were visualized by DIC optics and computer-enhanced video microscopy. In all cell models the transport of organelles was vectorial and saltatory in nature. The mean velocities for mitochondria, particles and nuclei were 1.4, 2.0, and 0.9 μm/s, respectively. Treatment with 10 μM nocodazole for 30 minutes caused a complete disappearance of microtubules and reversibly blocked directed transport of virtually all organelles, whereas cytochalasin D up to 20 μM was without effect. Correlative video and immunofluorescence microscopy of small fragments of wall-less mutant cells revealed a clear match between microtubule distribution and the tracks of moving organelles. We conclude that organelle movement in the filamentous fungus *Neurospora crassa* is a microtubule-dependent process.

Key words: microtubules, mitochondria, *Neurospora crassa*, organelle motility, protoplasts, wall-less fz;sg;os-1 mutant (SLIME)

INTRODUCTION

Numerous studies on the movement of organelles in animal cells have firmly established a central role for microtubules and associated force-generating molecules (Vale et al., 1985; Schroer et al., 1989; reviewed by Bloom, 1992), even though recent findings of actin-based motility in squid axon alert us to the need for caution in generalization (Kuznetsov et al., 1992). In contrast, in plant cells and some protists intracellular motility is believed to be driven by an actin-based force-generating system (Palevitz, 1976; Nothnagel et al., 1981; Sheetz and Spudich, 1983; Adams and Pollard, 1986; Kachar and Reese, 1988; Grolig, 1990; but see also Menzel and Schliwa, 1986). In fungi, however, the basic question of whether a force-generating system that drives organelle transport is based on microtubules (MTs), actin or some other cytoskeletal component is still unresolved. One cannot rule out the fact that the situation in fungi is more complex than that in animal cells (reviewed by McKerracher and Heath, 1987). For example, whereas several studies implicate MTs (Heath and Heath, 1978; Heath, 1988; Aist and Bayles, 1991), others suggest the presence of actomyosin-dependent force-generating mechanisms (Novick and Botstein, 1985; Kaminskyj et al., 1989; Heath and Kaminskyj, 1989). Concerning the movement of mitochondria, in particular, studies of germlings of *Aspergillus nidulans* (Oakley and Rinehart, 1985) and *Neurospora crassa* (Caesar-Ton That et al., 1988) argue against an involvement of MTs. The reason why even the basic mechanism is still unclear may in part be technical. Fungal cells are less tractable than most animal cells to studies of their motility, and the approaches that can be used are limited (Heath and Kaminskyj, 1989; Meyer et al., 1988). Many of the studies on mitochondrial and nuclear movement are based on indirect evidence derived from temporally separated 'snapshots' obtained by fluorescence and electron microscopy instead of direct observations.

Here we provide evidence, using cell models hitherto not employed in the study of the organelle transport machinery in fungi, that the vectorial movement of organelles in *N. crassa* is indeed a MT-dependent process. By removing the cell wall and preparing flat cell fragments it was possible to transform *Neurospora* cells into a cell model with features reminiscent of animal cells and to obtain a much clearer view of transport processes. These cell models made possible a high-resolution analysis of organelle transport under a variety of experimental conditions.

MATERIALS AND METHODS

Culture conditions

Neurospora crassa wild-type 74A (kindley provided by W. Neupert) was grown as described by Hennig and Neupert (1983). The wall-less fz;sg;os-1 strain of *N. crassa*, number FGSC 1118 (referred to as SLIME; Emerson, 1963), was obtained from the

Fungal Genetic Stock Center, Kansas City, USA, and was kindly provided by N. Pfanner. SLIME cells were grown in 50 ml culture medium (Smith and Scarborough, 1984) containing 50 μg/ml kanamycin A, at 30°C under continuous illumination and gentle shaking. For long-term culture the mutants were kept on 1% agar in culture medium. The liquid cultures were intiated from this stock or directly propagated by inoculation from other liquid cultures every 2 to 7 days.

Preparation of protoplasts and cell fragments

Protoplasts were generated from 14- to 16-hour-old hyphae or 8- to 10-hour-old germlings of *N. crassa* wild-type. A 14 ml sample of cell suspension was centrifuged at 150 ***g*** for 5 minutes and the loosely packed pellet (about 2 ml) was incubated with 5 mg/ml lysing enzymes (SIGMA) in PBS, pH 7.2, in a 30°C waterbath for 3 to 4 hours. To remove incompletely digested wall material the suspension was filtered through a 60 μm sieve and centrifuged for 10 minutes, at 80 ***g***, in an Eppendorf cup. The pellet was resuspended in 500 μl 10 mM Tris/200 mM sucrose, pH 7.0.

Cell fragments were prepared by coating coverslips with 25 μl of 10 mg/ml protamine sulfate (SIGMA) for 15 minutes in a wet chamber. After rinsing the coverslips twice with PHEM buffer (60 mM Pipes/20 mM Hepes/10 mM EGTA/2 mM $MgCl_2$; Schliwa and VanBlerkom, 1981), 100 μl of a suspension of SLIME in culture medium was placed on the coverslip and allowed to settle for 15 minutes. The coverslip was carefully dipped in PHEM buffer and pulled out at an angle. This generates shear forces large enough to remove the bulk of the cell bodies, leaving behind small, flattened droplets of cytoplasm that firmly adhere to the coverslip (cell fragments). The coverslip was then mounted on a slide so as to form the top of a flow-through chamber (Heath, 1988) and sealed with a mixture of equal parts of paraffin, vaseline and lanolin.

Light microscopy

Light and fluorescence microscopy were done using a ZEISS Axiophot microscope. Images were recorded with a Hamamatsu SCID C2400 camera, fed into a Hamamatsu DVS-1000 image processing system, and visualized on a Burle TC1119X black and white monitor. A Panasonic AG 6720 time-lapse video recorder was used to store the images on 1/2-inch video tape. To correlate the movement of mitochondria with the location of MTs as seen by immunofluorescence microscopy (IFM), individual cells were marked with a Leitz diamond marker after fixation. For photographic documentation the images were played back onto a high-resolution color monitor, FVM 1702 (Lucius and Baer) and photographs were taken with a Nikon SLR camera.

Quantitative and statistical analysis

For quantitative analyses, recorded images were reprocessed by passing over the Hamamatsu DVS 1000. Because of the complex behavioral repertoire of organelles, such as linear or curved path-

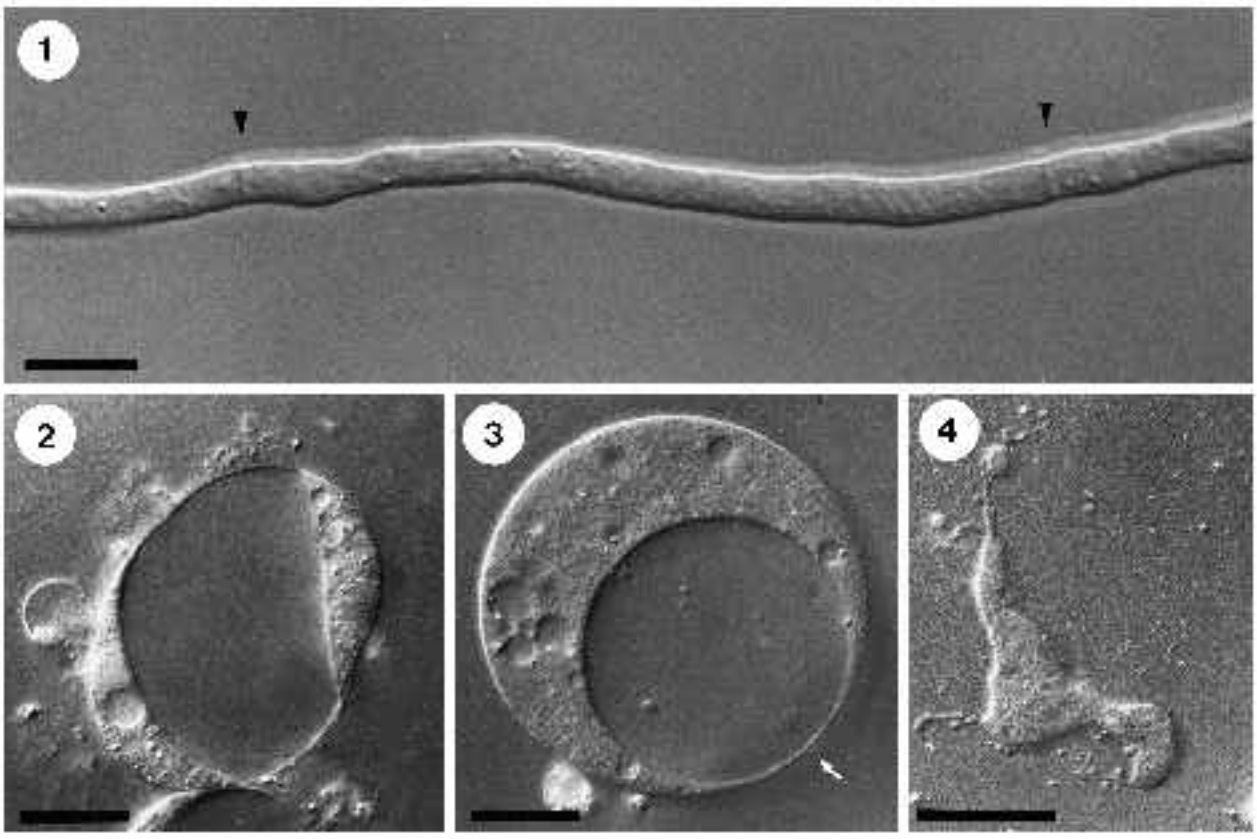

Figs 1-4. The different cell systems used in this study.
Fig. 1. A 16-hour-old vegetative hypha of *Neurospora crassa*; the cells are separated by septa (arrowheads). Bar, 15 μm.
Fig. 2. A 5-hour-old giant protoplast generated from 16-hour-old hyphae. Note the asymmetrical appearance and the big vacuole. Bar, 15 μm.
Fig. 3. A big wall-less cell of the fz;sg;oz-1 strain of *N. crassa*. The arrow marks the thin area above the vacuole. Figs 2 and 3 are optical sections through the middle portion of these spherical cells. Bar 15 μm.
Fig. 4. A flat cell fragment derived from SLIME attached to a protamine sulfate-coated coverslip. Bar, 15 μm.

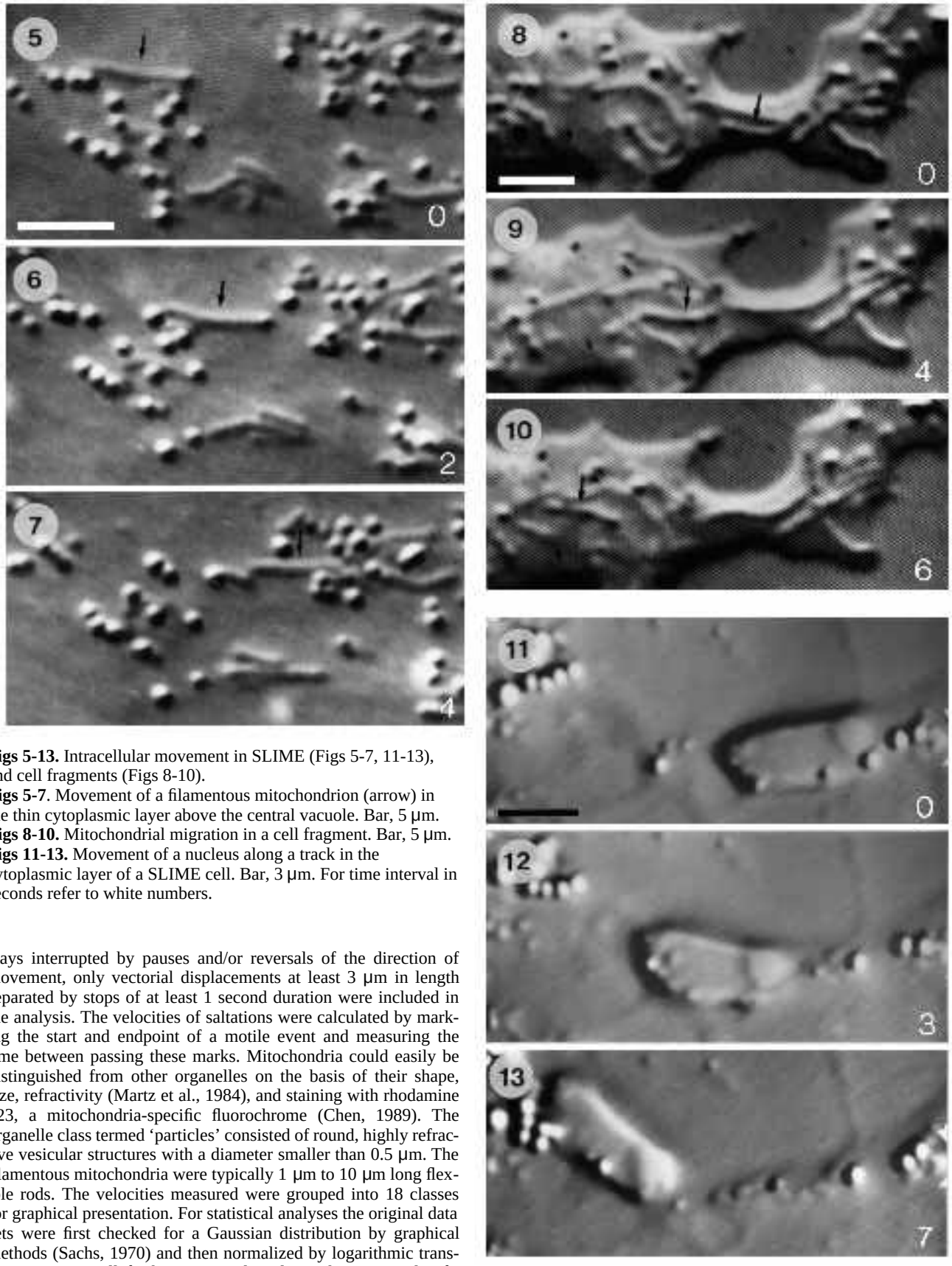

Figs 5-13. Intracellular movement in SLIME (Figs 5-7, 11-13), and cell fragments (Figs 8-10).
Figs 5-7. Movement of a filamentous mitochondrion (arrow) in the thin cytoplasmic layer above the central vacuole. Bar, 5 μm.
Figs 8-10. Mitochondrial migration in a cell fragment. Bar, 5 μm.
Figs 11-13. Movement of a nucleus along a track in the cytoplasmic layer of a SLIME cell. Bar, 3 μm. For time interval in seconds refer to white numbers.

ways interrupted by pauses and/or reversals of the direction of movement, only vectorial displacements at least 3 μm in length separated by stops of at least 1 second duration were included in the analysis. The velocities of saltations were calculated by marking the start and endpoint of a motile event and measuring the time between passing these marks. Mitochondria could easily be distinguished from other organelles on the basis of their shape, size, refractivity (Martz et al., 1984), and staining with rhodamine 123, a mitochondria-specific fluorochrome (Chen, 1989). The organelle class termed 'particles' consisted of round, highly refractive vesicular structures with a diameter smaller than 0.5 μm. The filamentous mitochondria were typically 1 μm to 10 μm long flexible rods. The velocities measured were grouped into 18 classes for graphical presentation. For statistical analyses the original data sets were first checked for a Gaussian distribution by graphical methods (Sachs, 1970) and then normalized by logarithmic transformation. For all further statistical analyses the statistical software packet SPSS was used. To clarify whether the mean values of the different data sets were equal, an ANOVA analysis was

carried out. Subsequently the single data sets were compared by a Fisher-LSD test at a level of significance of $\alpha = 0.05$. The mean velocities (Fig. 16) are the result of the backward transformation of the logarithmic mean. This treatment is recommended (Sachs, 1970) to reduce the distorting bias imposed by extremely high velocities.

Treatment with drugs

Drug experiments were done in the flow-through chamber under optical control. The spherical protoplasts and SLIME were held in place on the coverslip by covering them with a thin agar film of 2% agar/0.8% gelatin. Hyphae were attached on coverslips treated with 1 mg/ml poly-L-lysine. Cell fragments were generated on protamine sulfate-covered surfaces, as described above. The buffer was replaced by rinsing the chamber with 100 μl of 10 μM nocodazole or 2, 4 and 20 μM cytochalasin D/1% DMSO in 10 mM Tris/200 mM sucrose or PHEM buffer and the effects on the cells or fragments were recorded. The drugs were washed out by rinsing with buffer several times. As a control, 1% DMSO in PHEM was used and, in case of cytochalasin experiments, nocodazole treatment served as a positive control. Nocodazole experiments were done with hyphae, protoplasts, SLIME and cell fragments; the effect of cytochalsin was investigated in SLIME and cell fragments.

Immunolocalization of MTs and staining of actin

The immunocytochemistry of SLIME and cell fragments was done in the flow-through chamber under optical control. While recording the movement of organelles, the fixing solution, 0.5% glutaraldehyde/0.2% Triton X-100 in PHEM buffer or 3.5% formaldehyde/0.1% glutaraldehyde/0.2% Triton X-100 in PHEM buffer, was perfused through the chamber. The cells were fixed for 10 minutes and marked as described above. After rinsing the specimen with PHEM buffer and PBS, and treatment with sodium borohydride (2 mg/ml in PBS), the coverslips were incubated with monoclonal antibody YL 1/2 against yeast α-tubulin (Kilmartin et al., 1982) or WA 3 against bovine brain β-tubulin (made and provided by Dr U. Euteneuer). As second antibodies were used FITC-G rat in the case of YL and FITC-SAM mouse for WA 3. F-actin, a gift from Paul Janmey, was stained with rhodamine-phalloidin according to published procedures (Wulf et al., 1979).

RESULTS

Cell systems used

Vegetative hyphae of *Neurospora crassa* wild-type consisted of about 20-80 μm long cylindrical cells 3-6 μm in diameter (Fig. 1). They clearly showed fast movement of refractive particles, mostly along the length of the hyphae. Mitochondria were also seen to perform rapid, saltatory movements, but they were more difficult to follow, since their refractive index matched that of the dense cytoplasm, causing them to blend into the background. They were, however, clearly visualized after staining with R123 (Chen, 1989).

Protoplasts were about 15 to 20 μm in diameter and normally had a big vacuole (Fig. 2). While settling down in the hypo-osmotic buffer they may increase in size due to osmosis. Even larger cells (up to 60 μm in diameter) may result from protoplast fusion (Fig. 2). The bulk of the cytoplasm often formed a cap at one pole of the cell, with a thin layer of cytoplasm covering the vacuole. It was in this layer that particle and mitochondrial movements were best observed.

The cell wall-less mutant of *N. crassa* was similar in appearance to protoplasts (Fig. 3). The distinguishing features were a thicker layer of cytoplasm around the vacuole and larger numbers of mitochondria.

Cell fragments derived from SLIME were of different sizes and shapes (Fig. 4). In these flat residues sometimes less than 10 organelles were seen. Even in fragments as small as 22 μm × 14 μm, motility of mitochondria was seen (see Figs 27-29). As in SLIME, the mitochondria predominated in number and motility.

Characterization of intracellular motility

Saltatory movements of mitochondria occured in each of the four cell systems used, albeit to a different extent (Figs 5-7 and Figs 8-10). As a rule about half of the mitochondria showed vectorial movement (57.7% of 123 mitochondria in 6 SLIME cells moved within 1 minute), but many more seemed tethered to the cytosekeleton and showed reduced Brownian motion. The migration of mitochondria often consisted of a to and fro motion that sometimes gave way to quick continuous displacements of about 3 to 6 μm. We also observed slower stop and go migration without pauses of more than 1 second. In protoplasts and SLIME long mitochondria showed contortive and flexible movements typically observed for these organelles (Martz et al., 1984; Bereiter-Hahn, 1990).

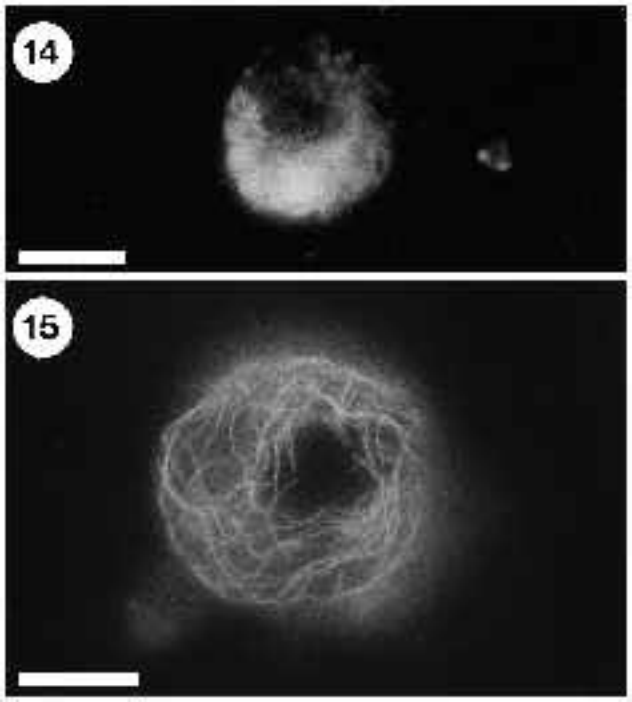

Figs 14 and 15. Fluorescence staining of F-actin and tubulin.
Fig. 14. Staining of F-actin with rhodamine-phalloidin in a SLIME cell. The staining is diffuse and patchy; no filament bundles are seen. Bar, 15 μm.
Fig. 15. Microtubules in the periphery of a SLIME cell. The unstained area could represent the central area above the vacuole, which often showed no intracellular motility. Bar, 15 μm.

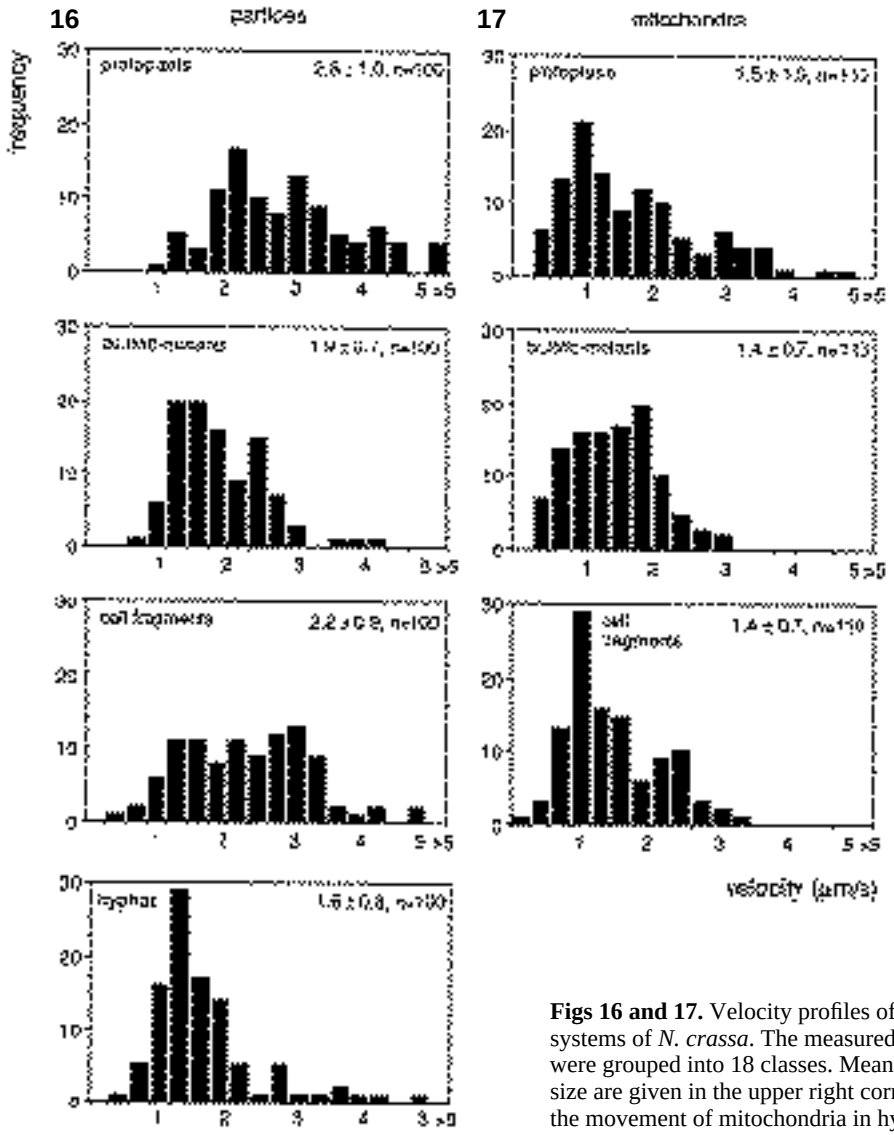

Figs 16 and 17. Velocity profiles of intracellular motility in the different cell systems of *N. crassa*. The measured velocities of particles and mitochondria were grouped into 18 classes. Mean velocity, standard deviation, and sample size are given in the upper right corner of each graph. As discussed in the text, the movement of mitochondria in hyphae was difficult to quantify.

The particles showed typical saltatory movement in each cell sytem; this form of intracellular motility dominated in hyphae and was hardly found in cell fragments. Saltations extended over distances of 5 µm to more than 10 µm, often with a change in direction but normally without a decrease in velocity. Occasionally we saw extremely fast movements of particles (up to 11 µm/s). Mitochondria and particles of different sizes usually followed the same invisible tracks; this was best seen in SLIME cells.

Apart from these organelles, very small particles barely detectable in video enhanced-differential interference contrast (VEC-DIC), as well as nuclei and vacuoles, took part in the intracellular motility, often sharing the same tracks with the more refractive particles. The very small particles moved significantly faster (3.2 ± 1.0 µm/s, n=100) than the bigger particles (Student's t-test, $P < 0.05$), whereas nuclear migration was relatively slow (0.9 ± 0.3 µm/s, n=13) and interrupted by long pauses (Figs 11-13). Vacuolar fragments were seen to move at about the same velocity as mitochondria (1.8 ± 0.8 µm/s, n=18). Because nuclear and vacuolar movement was observed rather infrequently compared to movement of vesicles and mitochondria, it was not included in the subsequent statistical analyses.

Statistical analysis of motility velocities

A statistical analysis using ANOVA demonstrated that the mean values of the velocity data sets are different (H_o, mean values are equal; degrees of freedom, 723; F-statisic value, 35,2383; $P < 0.001$) (see Figs 16, 17). The following Fisher-LSD test (H_o, compared mean velocities are equal; α, 0.05%) showed the mean mitochondria velocities to be a homogeneous group, different from the particle velocities. On the other hand, application of the same statistical method suggested that the mean particle velocities in the cell systems investigated are significantly different from each other (see Table 1). Whether there is a biologically relevant reason for this is unclear.

Drug treatment

In all cell systems tested, treatment with 10 µM nocodazole/0.06% DMSO led to a time-dependent cessation of the movement of particles and mitochondria. Within a few min-

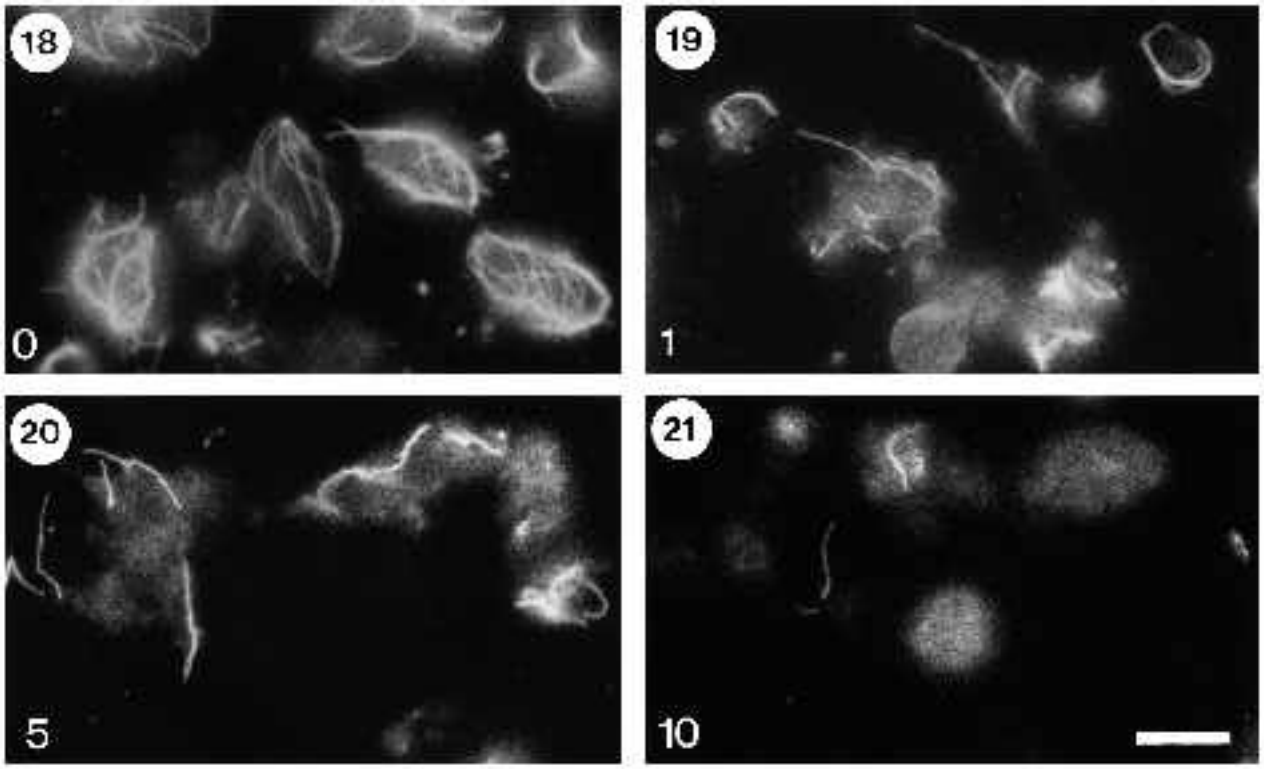

Figs 18-21. The effect of 10 μM nocodazole on cell fragments.
Fig. 18. Cell fragments generated from SLIME and attached on the coverslip showed long cytoplasmic MTs.
Fig. 19. After 1 minute of nocodazole treatment, many MTs were shorter than 7 μm and a few cell fragments lack MTs alltogether.
Fig. 20. After 5 minutes most of the cell fragments contained short (<7 μm) or just single long MTs.
Fig. 21. After 10 minutes of drug treatment most cell fragments were without MTs, and some cell fragments contained just single MTs.
The white numbers indicate the time of drug treatment in minutes. For a quantification of these observations, see Fig. 22. Bar, 10 μm.

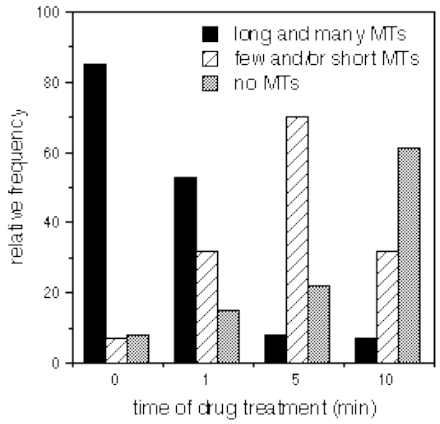

Fig. 22. The graph demonstrates the occurrence of MTs in cell fragments as a function of a time of nocodazole treatment. The intermediate state between 'long and many MTs' and 'no MTs' is characterized by the occurrence of MTs shorter than 7 μm and/or some single MTs longer than 7 μm. For each time point at least 150 cell fragments were analysed.

Table 1. Results of the Fisher-LSD test

	MF	MS	MP	PH	PS	PF	PP
MF							
MS							
MP							
PH	+	+					
PS	+	+	+	+			
PF	+	+	+	+	+		
PP	+	+	+	+	+	+	

First letter: M, mitochondria; P, particles.
Second letter: H, hyphae; P, protoplasts; S, SLIME; F, cell fragments.
+, The mean values are not equal.

utes we observed an increase in Brownian motion and a decrease in directed organelle motility until, after about 10 minutes, virtually all long-distance movement had ceased. This is in accordance with the observation that treatment with 10 μM nocodazole led to the disappearance of MTs in cell fragments (Figs 18-21 and Fig. 22). After rinsing the cells with buffer the motility of organelles recovered to normal levels within 10 minutes. In experiments with a SLIME cell we did two cycles of 10 μM nocodazole treatment and buffer rinsing, and determined the percentage of mitochondria moving within a 1 minute time window. At 10 minutes after adding nocodazole about 90% of the mitochondria (n=45) showed only Brownian motion and less than 10% clearly moved over only very short distances. One minute after rinsing with buffer the motility recovered to about 54% (n=46) and remained at about 49% after 7 minutes. After a second round of nocodazole treatment for 10 minutes mitochondrial motility decreased again to 8%

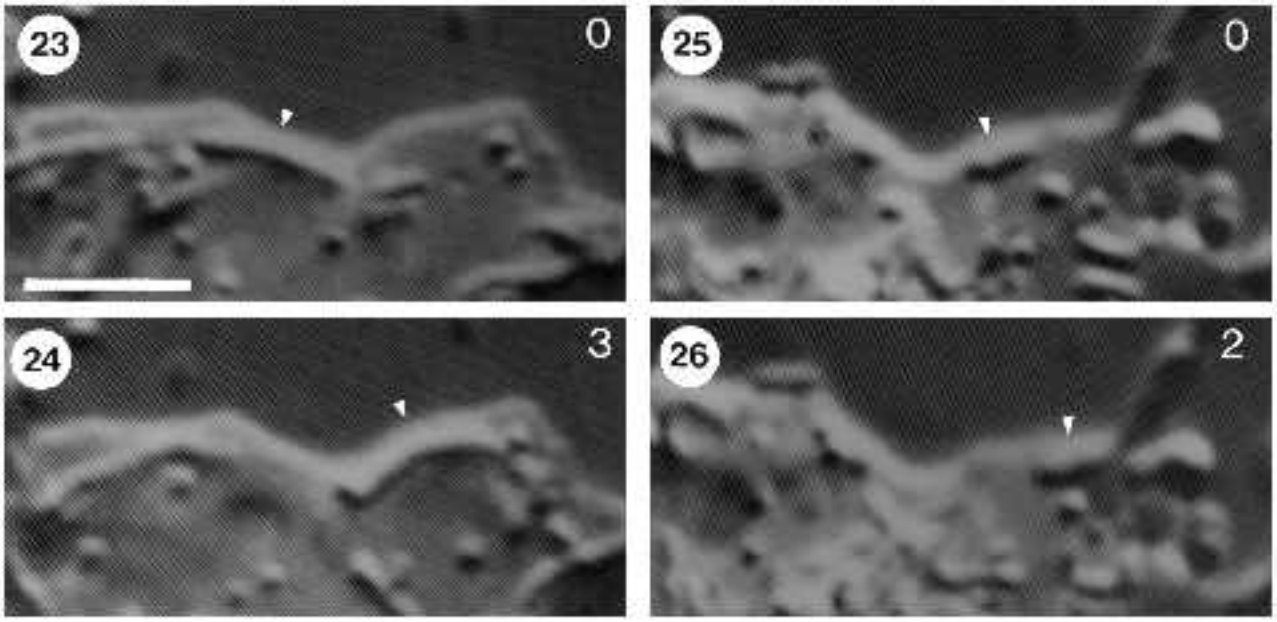

Figs 23-26. Treatment of a cell fragment with cytochalasin D.
Figs 23, 24. Movement of a filamentous mitochondrion along the edge of a cell fragment before treatment with cytochalsin D. Bar, 5 μm.
Figs 25, 26. The same edge after 50 minutes of drug treatment. Although the shape of the cell fragment changed slightly, small mitochondria (arrowhead) and particles still moved. For time interval in seconds refer to white numbers.

(*n*=35). The mean velocity in cells recovering from nocodazole treatment was similar to that of untreated cells (1.4 ± 0.6 μm/s). Likewise, in cell fragments the motility of mitochondria decreased from 90% to 10% after 2 minutes of drug treatment (*n*=23). Particle movement was affected in much the same way.

Cytochalasin D in concentrations up to 20 μM had no visible effect on intracellular motility (Figs 23-26). For example, 6 minutes after adding 4 μg/ml cytochalasin D/0.4% DMSO to a cell fragment, 47% of the mitochondria (*n*=17) in this cell fragment were in motion, and the proportion of moving mitochondria was about 57% (*n*=14) after 40 minutes. For reasons unknown, cytochalasin treatment led to increasing fragmentation of mitochondria in cell fragments, rendering quantification of their motility more difficult after longer exposure times.

Treatment with 1% DMSO for 30 minutes did not affect the intracellular motility, whereas nocodazole did stop organelle movement in cells that were unaffected by cytochalasin treatment. Thus the lack of effect of cytochalasin is not due to a lack of accessibility of the drug to the cells.

Immunolocalization of tubulin and fluorescent staining of actin

Neither in SLIME nor in cell fragments did rhodamine-phalloidin label actin bundles or other organized arrays of actin. The only fluorescence staining of actin seen was a diffuse cloudy accumulation in SLIME (Fig. 14). The lack of filamentous structures in SLIME was probably not an artifact due to the staining procedure, since our batch of rhodamine-phalloidin was capable of correctly binding to F-actin in vitro (data not shown).

In contrast, cytoplasmic MTs were clearly visible. The best labelling was achieved with the WA 3 antibody against bovine brain β-tubulin (Fig. 15). Long MTs coursed through the periphery of the spherical SLIME cells without any discernible order. Detailed analyses of the cell fragments generated from SLIME allowed a clear, positive correlation between the presence and distribution of MTs and the occurrence of organelle motility: first, all fragments (*n*=27) that showed directed movement of organelles also contained MTs, whereas those that did not (*n*=10) were free of MTs; second, in those fragments that did contain MTs, the course of the MTs showed a reasonably good correlation with the path of mitochondrial movement (Figs 27-32).

DISCUSSION

The movement of mitochondria and other organelles was observed with computer contrast-enhanced DIC in four cell models of *N. crassa* under different experimental conditions, and their tracks of motion were compared directly with the positions of MTs as seen by immunofluorescence microscopy. We show that mitochondrial movement was dependent upon, and mediated by, cytoplasmic microtubules, and that F-actin played no detectable role in this process. Other organelles, such as nuclei and a variety of vesicular organelles, frequently use the same tracks as mitochondria, but move at different rates.

Whereas several studies demonstrate the presence of both MTs (Hoch and Staples, 1985; McKerracher and Heath, 1987; Runeberg et al., 1986; Roos and Turian, 1977; Salo et al., 1989; Temperli et al., 1990) and actin filaments (Heath, 1987, 1988; Hoch and Staples, 1983, 1985; Tucker et al., 1986; Runeberg et al., 1986; Barja et al., 1991) in

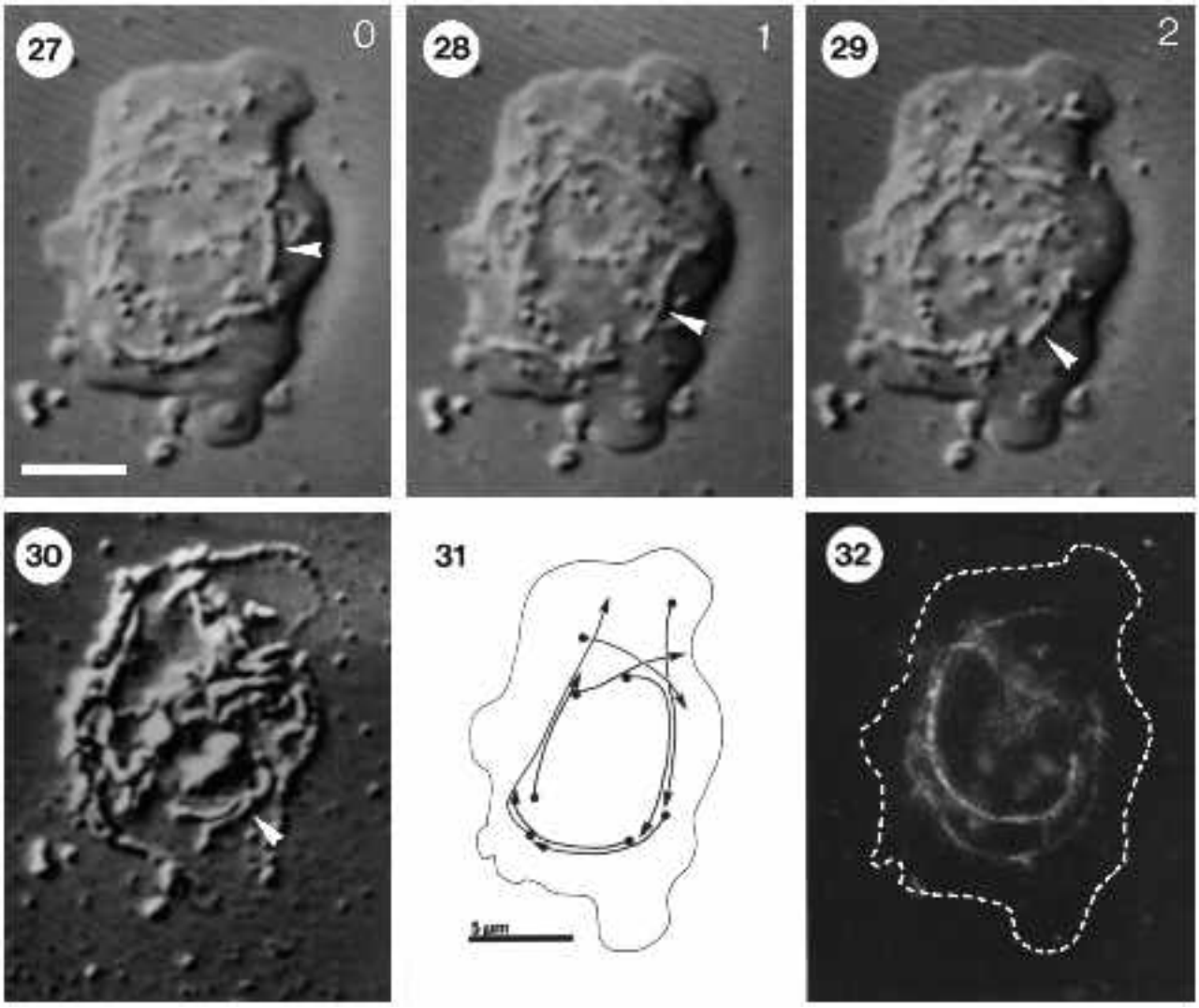

Figs 27-32. The correlation between mitochondrial motion tracks and cytoplasmic microtubules in a small cell fragment.
Figs 27-29. Movement of mitochondria (arrowhead) in a cell fragment. For time interval in seconds refer to white numbers. Bar, 5 μm.
Fig. 30. The same cell fragment after rapid lysis and fixation. Mitochondria are frozen in their motion and their remnants decorate the motion tracks (arrowhead).
Fig. 31. The graph shows the movements of mitochondria within a 25 second time interval preceding fixation. Interestingly, all mitochondria move in one direction.
Fig. 32. Localization of immunostained microtubules. Note the close correspondence between the mitochondrial motion tracks and the distribution of MTs.

several species of fungi, the problem of whether MTs or actin, or both, are involved in organelle transport has remained unresolved (for a thoughtful and thorough review, see McKerracher and Heath, 1987). An involvement of MTs has been invoked on the basis of direct observations by light microscopy, ultrastructural observations of cross-bridges between MTs and organelles, and pharmacological studies (Howard and Aist, 1979; Raudaskoski et al., 1988; Aist and Bayles, 1991; Howard, 1983). On the other hand, certain types of vesicle or organelle motility are proposed to be independent of MTs (Hoch et al., 1987; Caesar-Ton That et al., 1988; Herr and Heath, 1982; Oakley and Rinehart, 1985), leading to the suggestion that some organelles may move along actin filaments (Heath and Kaminskyj, 1989). Finally, it has been suggested that organelle movements may require co-extensive arrays of both MTs and actin filaments (Heath et al., 1982; Hoch and Staples, 1985; summarized by Heath, 1990).

The observations on four cell models of *N. crassa* presented here showed organelles to move in a saltatory manner only in association with MTs. There was a positive correlation between the presence of MTs and the occurrence of organelle movements. This was particularly apparent in the cell fragments derived from SLIME, where only those fragments that contain MTs also exhibit directional transport. Moreover, there was a congruence between the tracks of moving organelles and the paths of microtubules. This congruence was not perfect, perhaps as a result of MT rearrangements and/or assembly/disassembly during the period of observation (e.g. 25 seconds, for the fragment

shown in Figs 22-27). Finally, the drug studies performed here are consistent with the view that organelles in *N. crassa* move in a MT-dependent, not an actin-dependent, manner. Though we cannot formally exclude the possibility that a subset of actin filaments associated with organelle-propelling MTs are involved, we find this unlikely, on the basis of an analogy with the amoeba, *Reticulomyxa filosa*, in which actin filaments and MTs are co-extensive, yet organelle transport is driven by a MT motor and does not require the presence of actin (Koonce and Schliwa, 1986; Euteneuer et al., 1988).

One might argue that the transport observed in the cell wall-less models used here is not representative of the transport processes in intact hyphae. We find this unlikely on the following grounds: first, the behavior of particles in hyphae and cell fragments was very similar, even though the average velocities may vary. The same applies to mitochondrial movement in protoplasts, SLIME and cell fragments. In addition, these organelles moved with about equal velocities. Second, it is hard to believe that during the short time it takes to generate protoplasts from hyphae, the mechanism of organelle transport would change radically. We cannot entirely exclude the possibility, however, that the stress of protoplast formation has adverse effects on organelle motility. This seems rather unlikely, since the behavior of organelles in SLIME is virtually indistinguishable from that in protoplasts. Third, even though a SLIME cell looks very different from a hyphal cell, it nevertheless is a functioning fungal cell capable of growth and reproduction.

The movements of organelles observed here might be driven by a MT-dependent motor molecule such as kinesin or cytoplasmic dynein, representatives of which have been identified in a variety of 'lower' eukaryotes, including yeast (Meluh and Rose, 1990; Hagan and Yanagida, 1990), *Aspergillus nidulans* (Enos and Morris, 1990), *Dictyostelium* (McCaffrey and Vale, 1989), *Acanthamoeba castellanii* (Kachar et al., 1987), and *Reticulomyxa* (Euteneuer et al., 1988). At the very least, our studies suggest that *N. crassa* must possess all the molecular components necessary to support vectorial transport along MTs. While our data do not rule out a role for actin, they strongly implicate microtubule-dependent motors in the movements of organelles visualized here. In this context, it is worth noting that we have identified a microtubule-dependent motor activity in *Neurospora* cytoplasmic extracts. The characterization of this motor in *Neurospora*, which may well drive organelle movements, represents a challenge for the future.

We thank Diedrik Menzel for carefully reading the manuscript and his helpful suggestions, and Dr Harald Mathes for his help with the statistics. The authors' research is supported by the Deutsche Forschungsgemeinschaft.

REFERENCES

Adams, R. J. and Pollard, T. D. (1986). Propulsion of organelles isolated from Acanthamoeba along actin filaments by myosin 1. *Nature* **322**, 754-756.

Aist, J. R. and Bayles, C. J. (1991). Organelle motility within mitotic asters of the fungus Nectaria haematococca. *Eur. J. Cell Biol.* **56**, 358-363.

Barja, F., Nguyen, B.-N. and Turian, G. (1991). Localization of actin and characterization of its isoforms in the hyphae of Neurospora crassa. *FEMS Microbiol. Lett.* **77**, 19-24.

Bereiter-Hahn, J. (1990). Behavior of mitochondria in the living cell. *Int. Rev. Cytol.* **122**, 1-63.

Bloom, G. S. (1992). Motor proteins for cytoplasmic microtubules. *Curr. Opin. Cell Biol.* **4**, 66-73.

Caesar-Ton That, T. C., Rossier, C., Barja, F., Turian, G. and Roos, U.-P. (1988). Induction of multiple germ tubes in Neurospora crassa by antitubulin agents. *Eur. J. Cell Biol.* **46**, 68-79.

Chen, L. B. (1989). Fluorescent labelling of mitochondria. *Meth. Cell Biol.* **29**, 103-123.

Emerson, S. (1963). Slime, a plasmodioid variant of Neurospora crassa. *Genetica* **34**, 162-182.

Enos, A. and Morris, N. R. (1990). Mutation of a gene that encodes a kinesin-like protein blocks nuclear division in *A. nidulans*. *Cell* **60**, 1019-1027.

Euteneuer, U., Koonce, M. P., Pfister, K. K. and Schliwa, M. (1988). An ATPase with properities expected for the organelle motor of the giant amoeba Reticulomyxa. *Nature* **332**, 176-178.

Grolig, F. (1990). Actin-based organelle movements in interphase Spirogyra. *Protoplasma* **155**, 29-42.

Hagan, I. and Yanagida, M. (1990). Novel potential mitotic motor protein encoded by the fission yeast cut7+ gene. *Nature* **347**, 563-567.

Heath, I. B. (1987). Preservation of labile cortical array of actin filaments in growing hyphal tips of the fungus Saprolegnia ferax. *Eur. J. Cell Biol.* **44**, 10-16.

Heath, I. B. (1988). Evidences against a direct role for cortical actin arrays in saltatory organelle motility in hyphae of the fungus *Saprolegnia ferax*. *J. Cell Sci.* **91**, 41-47.

Heath I. B. (1990). The roles of actin in tip growth of fungi. *Int. Rev. Cytol.* **123**, 95-127.

Heath, I. B. and Heath, M. C. (1978). Microtubules and organelle movements in the rust fungus Uromyces phaseoli var vignae. *Cytobiology* **16**, 393-411.

Heath, I. B., Heath, M. C. and Herr, F. (1982). Motile systems in fungi. In *Prokaryotic and Eukaryotic Flagella*. 35th Symposium of the Society for Experimental Biology (ed. W. B. Amos and J. G. Dukett), pp. 563-588. Cambridge University Press, Cambridge.

Heath, I. B. and Kaminskyj, S. G. W. (1989). The organization of tip-rowth related organelles and microtubules revealed by quantitative analysis of freeze-substituted oomycete hyphae. *J. Cell Sci.* **93**, 41-52.

Henning, B. and Neupert, W. (1983). Biogenesis of cytochrome *c* in Neurospora crassa. *Meth. Enzymol.* **97**, 261-274.

Herr, F. B. and Heath, M. C. (1982). The effects of antimicrotuuble agents on organelle positioning in the cowpea rust fungus Uromyces phaseoli var. vignae. *Exp. Mycol.* **6**, 15-24.

Hoch, H. C. and Staples, R. C. (1983). Visualization of actin in situ by rhodamine-conjugated phalloin in the fungus Uromyces phaseoli. *Eur. J. Cell Biol.* **32**, 52-58.

Hoch, H. C. and Staples, R. C. (1985). The microtubule cytoskeleton in hyphae of Uromyces phaseoli germlings: Its relationship to the region of nucleation and to the F-actin cytoskeleton. *Protoplasma* **124**, 112-122.

Hoch, H. C., Tucker, B. E. and Staples, R. C. (1987). An intact microtubule cytoskeleton is necessary for mediation of the signal for cell differentation in Uromyces. *Eur. J. Cell Biol.* **45**, 209-218.

Howard, R. J. (1983). Cytoplasmic transport in hyphae of Gilbertella. *Mycol. Soc. Amer. Newslett.* **34**, 24.

Howard, R. J. and Aist, J. R. (1979). Hyphal tip cell ultrastructure of the fungus Fusarium: Improved preservation by freeze-substitution. *J. Ultrastruct. Res.* **66**, 224-234.

Kachar, B., Albanesi, J. P., Fujisaki, H. and Korn, E. D. (1987). Extensive purification from Acanthamoeba castellanii of a microtubule-dependent translocator with microtubule-activated Mg^{2+}-ATPase activity. *J. Biol. Chem.* **262** (33), 16180-16185.

Kachar, B. and Reese, T. S. (1988). The mechanism of cytoplasmic streaming in characean algal cells: sliding of endoplasmic reticulum along actin filaments. *J. Cell Biol.* **106**, 1545-1552.

Kaminskyj, S. G. W., Yoon, K. S. and Heath, I. B. (1989). Cytoskeletal interactions with post-mitotic migrating nuclei in the oyster mushroom

fungus, Pleurotus ostreatus: evidences against a force-generating role of astral microtubules. *J. Cell Sci.* **94**, 663-674.

Kilmartin, J. V., Wright, B and Milstein, C. (1982). Rat monoclonal antibodies derived by using a new nonsecreting rat cell line. *J. Cell Biol.* **93**, 576-582.

Koonce, M. P. and Schliwa, M. (1986). Reactivation of organelle movements of cytoskeletal framework of a giant freshwater amoeba. *J. Cell Biol.* **103**, 605-612.

Kuznetsov, S. A., Langford, G. M. and Weiss, D. G. (1992). Actin dependent organelle movement in squid axoplasm. *Nature* **356**, 722-725.

Martz, D., Lasek, R. J., Brady, S. T. and Allen, R. D. (1984). Mitochondrial motility in axons: Membranous organelles may interact with the force generating systems through multiple surface binding sites. *Cell Motil.* **4** (89), 89-101.

McCaffrey, G. and Vale, R. D. (1989). Identification of a kinesin-like microtubule-based motor protein in Dictyostelium discoideum. *EMBO J.* **8** (11), 3229-3234.

McKerracher, L. J. and Heath, I. B. (1987). Topical review: cytoplasmic migration and intracellular organelle movements during tip growth of fungal hyphae. *Exp. Mycol.* **11**, 79-100.

Meluh, P. B. and Rose, M. D. (1990). KAR3, a kinesin-related gene required for yeast nuclear fusion. *Cell* **60**, 1029-1041.

Menzel, D. and Schliwa, M. (1986). Motility in the siphonous green alga Bryopsis. II. Chloroplast movement requires both microtubules and actin filaments. *Eur. J. Cell Biol.* **40**, 286-296.

Meyer, S. L. F., Kaminskyj, S. G. W. and Heath, I. B. (1988). Nuclear migration in a nud mutant of *Aspergillus nidulans* is inhibited in the presence of a quantitatively normal population of cytoplasmic microtubules. *J. Cell Biol.* **106**, 773-778.

Nothnagel, E. A., Barak, L. S., Sanger, J. W. and Webb, W. W. (1981). Fluorescence studies on the modes of cytochalasin B and phallotoxin action on cytoplasmic streaming in Chara. *J. Cell Biol.* **88**, 364-372.

Novick, P. and Botstein, D. (1985). Phenotypic analysis of temperature-sensitive yeast actin mutants. *Cell* **40**, 405-416.

Oakley, B. R. and Rinehart, J. E. (1985). Mitochondria and nuclei move by different mechanisms in *Aspergillus nidulans. J. Cell Biol.* **101**, 2392-2397.

Palevitz, B. A. (1976). Actin cables and cytoplasmic streaming in green plants. In *Cell Motility* (ed. R. Goldmann, I. Pollard and J. Rosenbaum), Cold Spring Harbor Conference on Cell Proliferation, Cold Spring Harbor Laboratory, NY.

Raudaskoski, M., Salo, V. and Niini, S. S. (1988). Structure and function of the cytoskeleton in filamentous fungi. *Karstenia* **28**, 49-60.

Roos, U.-P. and Turian, G. (1977). Hyphal tip organization in Allomyces arbuscula. *Protoplasma* **93**, 231-247.

Runenberg, P., Raudaskoski, M. and Virtanen, I. (1986). Cytoskeletal elements in the hyphae of the homobasidiomycete Schizophyllum commune visualized with indirect immunofluorescence and NBD-phallacidin. *Eur. J. Cell Biol.* **41**, 25-32.

Sachs, L. (1970). *Statistische Methoden, ein Soforthelfer*. Springer, Berlin, Heidelberg, New York.

Salo, V., Niini, S. S., Virtanen, I. and Raudaskoski, M. (1989). Comparative immunocytochemistry of cytoskeleton in filamentous fungi with dikaryotic and multinucleate hyphae. *J. Cell Sci.* **94**, 11-24.

Schliwa, M. and VanBlerkom, J. (1981). Structural interaction of cytoskeletal components. *J. Cell Biol.* **90**, 222-235.

Schroer, T. A., Steuer, E. R. and Sheetz, M. P. (1989). Cytoplasmic dynein is a minus end-directed motor for membranous organelles. *Cell* **56**, 937-946.

Sheetz, M. P. and Spudich, J. A. (1983). Movement of myosin-coated fluorescent beads on actin cables in vitro. *Nature* **303**, 31-35.

Smith, R. and Scarborough, G. A. (1984). Large-scale isolation of Neurospora plasma membrane H^+-ATPase. *Anal. Biochem.* **138**, 156-163.

Temperli, E., Roos, U. P. and Hohl, H. R. (1990). Actin and tubulin cytoskeletons in the germlings of the oomycete fungus Phytophora infestans. *Eur. J. Cell Biol.* **53**, 75-88.

Tucker, B. E., Hoch, H. C. and Staples, R. C. (1986). The involvement of F-actin in Uromyces cell differentiation: The effects of cytochalasin E and phalloidin. *Protoplasma* **135**, 88-101.

Vale, R. D., Reese, T. S. and Sheetz, M. P. (1985). Identification of a novel force-generating protein, kinesin, involved in microtubule-based motility. *Cell* **42**, 39-50.

Wulf, E., Deboben, A., Bantz, F. A., Faulstich, H. and Wieland, T. (1979). Fluorescent phallotoxin, a tool for visualization of cellular actin. *Proc. Nat. Acad. Sci. USA* **76**. 4498-4502.

(Received 22 December 1992 - Accepted, in revised form, 6 July 1993)